Coregistration Based on Three Parts of Two Complex Images and Contoured Windows for Synthetic Aperture Radar Interferometry

Qifeng Yu, Sihua Fu, Helmut Mayer, Xiaolin Liu, and Xia Yang

***Abstract*—The coregistration of complex image pairs is a very important step in synthetic aperture radar interferometry (InSAR) data processing. This letter proposes a novel coregistration method that only needs three arbitrary parts of the two complex images instead of four parts in the existing coregistration methods. This method constitutes an integrated three-part method for InSAR data processing with our contoured-correlation-interferometry method for phase-image generation. Saving one part transmission makes a significant advantage when processing SAR images on satellites. Furthermore, we demonstrate that, by means of using fringe contoured windows instead of squared windows, the accuracy of the coregistration for both the three-part coregistration method and the existing methods can be improved considerably.**

***Index Terms*—Coherence, contoured window, coregistration, correlation, synthetic aperture radar interferometry (InSAR).**

I. Introduction

SYNTHETIC aperture radar interferometry (InSAR), a technique under fast development, is used widely for measuring the topography of a surface, its changes over time, and changes of the characteristics of a surface [1]. With two spatially separated antennas, InSAR performs two imaging processes over the same area producing two complex images containing phase data related to range direction. Phase differences are obtained after the interference of the two complex images, and based on them, digital elevation models (DEM) can be generated. Compared with the traditional photogrammetry, InSAR has the advantages to produce the DEM with high resolution over large areas independently of lighting conditions and weather.

Precise coregistration remains one of the critical elements to improve the accuracy of the surface-elevation measurement. In general, high subpixel coregistration accuracy is needed to obtain stable interference patterns [2]. There are three common measures used to evaluate the quality of the coregistration of the two complex images: 1) coherence of the two complex images is the most commonly used [3]; 2) signal-to-noise ratio of the phase difference image of the two complex images [4]; and 3) an average fluctuation function of the difference image of the two complex images [2]. A single-look complex image pair is composed of four parts: two real and two imaginary parts. Existing methods require all four parts of the complex image pair to conduct precise coregistration.

We have proposed a method termed "contoured correlation interferometry" (CCI) to generate speckle-noise-reduced phase images for InSAR image processing [5]. An important advantage of the CCI method is that it needs only three arbitrary parts of the two complex images rather than four for the conventional conjugate-multiplication method. Saving one image transmission from four is a significant advantage when processing SAR images on satellites.

The main idea of CCI method is as follows: The correlations are performed among the real and imaginary parts of the coregistered complex image pair to measure the data similarity. The similarities generate the new phase image that has the same phase field as that as derived by the conjugate-multiplication method but almost without the decorrelation noise. First, we correlate one real part and one imaginary part from the two coregistered complex images within fringe contoured windows for every resolution cell, resulting in a mostly speckle-free sine fringe image. Then, another correlation is performed between the two real parts or the two imaginary parts of the two complex images, resulting in a cosine fringe image. Finally, the phase image is generated by the arctan function for the ratio of the sine and the cosine images.

Fringe contoured window is an approximate equal-phase window, in which the phase value of every resolution cell is almost the same. The size of the window varies according to the fringe-density and curvature of the interferogram. When the fringe is sparse and is of little curvature, larger window size is selected, and vice versa. The details to determine fringe contoured windows can be found in [5] and [6].

In [5], we did not discuss the coregistration process of the two complex images used. If the common coregistration methods that require all four parts of the two complex images are used, the advantage that the CCI needs only three parts becomes less important. To make full use of this feature of CCI, we propose a measure for coregistration of the two interfering SAR images that requires only three arbitrary parts of the two complex images which can be the same as used by CCI. We term it the

Manuscript received August 12, 2006; revised December 21, 2006.

Q. Yu is with the College of Optical Engineering and the College of Aerospace Engineering, National University of Defense Technology, Changsha 410073, China (e-mail: yuqifeng@vip.sina.com).

S. Fu, X. Liu, and X. Yang are with the College of Aerospace Engineering, National University of Defense Technology, Changsha 410073, China.

H. Mayer is with the Institute of Photogrammetry and Cartography, Bundeswehr University, 85577 Munich, Germany.

Digital Object Identifier 10.1109/LGRS.2007.894146

"three-part method." It allows taking three arbitrary parts, i.e., two real parts and one imaginary part, and vice versa, to register the SAR image pair, to generate the phase image, as well as for the rest of the processing, which we believe is a markedly different solution to InSAR data processing.

Furthermore, we propose to replace the square window in common coregistration methods by fringe contoured window to more precisely register the complex image pair.

II. Principle of the New Registration Method

For InSAR, two complex images of the same scene are obtained by repeat-pass SAR imaging:

$$\begin{aligned} V_1(r,x) &= A_1 e^{i\phi_1} = A_1 \cos\phi_1 + iA_1 \sin\phi_1 \\ &= A_1\cos(\phi_{1c}+u_1) + iA_1\sin(\phi_{1c}+u_1) \\ &= a_1 + b_1 i \end{aligned} \tag{1}$$

$$\begin{aligned} V_2(r,x) &= A_2 e^{i\phi_2} \\ &= A_2\cos(\phi_{2c}+u_2) + iA_2\sin(\phi_{2c}+u_2) \\ &= a_2 + b_2 i \end{aligned} \tag{2}$$

where r and x represent the range direction and the azimuth direction coordinate, A_1 and A_2, are the amplitudes of the complex data, and ϕ_1 and ϕ_2 are response wave phases of the two antennas with random speckle noise. ϕ_1 and ϕ_2 include two parts: one are the propagation-induced phase terms ϕ_{1c} and ϕ_{2c} proportional to the range, and the other are uncertain phase or scattering phase terms, u_1 and u_2, corresponding to random speckle, i.e., $\phi_1 = \phi_{1c} + u_1$ and $\phi_2 = \phi_{2c} + u_2$. For the sake of convenience, we call $V_1(r,x)$ as the master image and $V_2(r,x)$ as the slave image. Formula deduction of our coregistration measure is as follows.

The correlation formula between functions f_1 and f_2 is

$$C(r,x) = \frac{\langle f_1 \cdot f_2\rangle_{m\times n}}{\sqrt{\langle f_1^2\rangle_{m\times n}\cdot\langle f_2^2\rangle_{m\times n}}} \tag{3}$$

where operator $\langle\cdot\rangle_{m\times n}$ stands for the calculation of the average of a variable for $m\times n$ pixels.

First, we correlate the real part of the master image with the real part of the slave image and compute their respective automatic correlations:

$$\begin{aligned} &\langle a_1\ a_2\rangle_{m\times n} \\ &\quad = \langle A_1\cos(\phi_{1c}+u_1)\cdot A_2\cos(\phi_{2c}+u_2)\rangle_{m\times n} \\ &\quad = \left\langle \frac{1}{2}A_1A_2\cdot[\cos(\phi_{1c}+\phi_{2c}+u_1+u_2) \right. \\ &\qquad\qquad \left. +\cos(\phi_{1c}-\phi_{2c}+u_1-u_2)]\right\rangle_{m\times n} \end{aligned} \tag{4}$$

$$\begin{aligned} &\langle a_1\ a_1\rangle_{m\times n} \\ &\quad = \langle A_1\cos(\phi_{1c}+u_1)\cdot A_1\cos(\phi_{1c}+u_1)\rangle_{m\times n} \\ &\quad = \left\langle \frac{1}{2}A_1A_1\cdot[\cos(\phi_{1c}+\phi_{1c}+u_1+u_1) \right. \\ &\qquad\qquad \left. +\cos(\phi_{1c}-\phi_{1c}+u_1-u_1)]\right\rangle_{m\times n} \\ &\quad = \frac{1}{2}\langle A_1A_1\rangle_{m\times n}\cdot\langle 1+\cos(2\phi_{1c}+2u_1)\rangle_{m\times n} \end{aligned} \tag{5}$$

$$\begin{aligned} &\langle a_2\ a_2\rangle_{m\times n} \\ &\quad = \frac{1}{2}\langle A_2A_2\rangle_{m\times n}\cdot\langle 1+\cos(2\phi_{2c}+2u_2)\rangle_{m\times n}. \end{aligned} \tag{6}$$

In a previous deduction, since the phase and the magnitude are uncorrelated, the following assumption has been made [7]:

$$\begin{aligned} &\langle A_i\cdot A_j\cdot\cos\phi_i\cdot\cos\phi_j\rangle_{m\times n} \\ &\qquad = \langle A_i\cdot A_j\rangle_{m\times n}\cdot\langle\cos\phi_i\cdot\cos\phi_j\rangle_{m\times n}. \end{aligned} \tag{7}$$

u_1 and u_2 are both random speckle variables. According to speckle-statistic theory [8], for a window with size $m\times n$, large enough (according to our experience, the window size should be larger than $m\times n = 25$) to hold for a random variable u_i

$$\langle\cos u_i\rangle_{m\times n} = \langle\sin u_i\rangle_{m\times n} = 0 \qquad (i=1,2). \tag{8}$$

Then, supposing that ϕ_{1c} and ϕ_{2c} are constant, which is true on our fringe contoured window that is a curve coinciding with the local fringe contour with a width of m, it results is on the fringe contoured windows:

$$\begin{aligned} &\langle\cos(\phi_{1c}+\phi_{2c}+u_1+u_2)\rangle_{m\times n} \\ &\quad = \langle\cos(\phi_{1c}+\phi_{2c})\cdot\cos(u_1+u_2) \\ &\qquad\quad -\sin(\phi_{1c}+\phi_{2c})\cdot\sin(u_1+u_2)\rangle_{m\times n} \\ &\quad = \cos(\phi_{1c}+\phi_{2c})\cdot\langle\cos(u_1+u_2)\rangle_{m\times n} \\ &\qquad\quad -\sin(\phi_{1c}+\phi_{2c})\cdot\langle\sin(u_1+u_2)\rangle_{m\times n} \\ &\quad = 0. \end{aligned} \tag{9}$$

Using (8) and (9) and substituting (4)–(6) into (3) yields (10), shown at the bottom of the next page. In the same way, we correlate the real part of the master image with the imaginary part of the slave image and obtain

$$C_2 = \frac{\langle A_1A_2\rangle_{m\times n}}{\sqrt{\langle A_1^2\rangle_{m\times n}\cdot\langle A_2^2\rangle_{m\times n}}}\cdot\langle -\sin(\Delta\phi_c+\Delta u)\rangle_{m\times n}. \tag{11}$$

The coregistration measure of our method is proposed in the following form:

$$\begin{aligned} g &= \sqrt{C_1^2 + C_2^2} \\ &= \frac{|\langle A_1 A_2 \rangle_{m\times n}|}{\sqrt{\langle A_1^2 \rangle_{m\times n} \cdot \langle A_2^2 \rangle_{m\times n}}} \\ &\quad \cdot \sqrt{\langle \cos(\Delta\phi_c + \Delta u)\rangle_{m\times n}^2 + \langle \sin(\Delta\phi_c + \Delta u)\rangle_{m\times n}^2}. \end{aligned} \tag{12}$$

On the other hand, if we directly substitute $V_1(r,x)$ and $V_2(r,x)$ in (3), the conventional coregistration measure of coherence is derived:

$$\begin{aligned} \rho &= \frac{\left| \sum_{r=1}^{M} \sum_{x=1}^{N} V_1(r,x) \cdot V_2^*(r,x) \right|}{\sqrt{\sum_{r=1}^{M} \sum_{x=1}^{N} |V_1(r,x)|^2 \cdot \sum_{r=1}^{M} \sum_{x=1}^{N} |V_2(r,x)|^2}} \\ &= \frac{|\langle A_1 A_2 \rangle_{m\times n}| \cdot \left| \left\langle e^{i(\phi_{1c} - \phi_{2c} + u_1 - u_2)} \right\rangle_{m\times n} \right|}{\sqrt{\langle A_1^2 \rangle_{m\times n} \cdot \langle A_2^2 \rangle_{m\times n}}} \\ &= \frac{|\langle A_1 A_2 \rangle_{m\times n}|}{\sqrt{\langle A_1^2 \rangle_{m\times n} \cdot \langle A_2^2 \rangle_{m\times n}}} \\ &\quad \cdot \sqrt{\langle \cos(\Delta\phi_c + \Delta u)\rangle_{m\times n}^2 + \langle \sin(\Delta\phi_c + \Delta u)\rangle_{m\times n}^2}. \end{aligned} \tag{13}$$

It is no other than the correlation expression in the study in [9]. Equations (12) and (13) demonstrate that our coregistration quality-evaluation criterion of g is equivalent mathematically to the conventional coherence measure ρ. However, all four parts (i.e., both real and both imaginary parts of the two complex images) are necessary if we use (13) to compute ρ. In contrast, only three arbitrary parts of the two complex images, rather than four, are needed if we adopt (12) to calculate g, which can be seen clearly from the formula deduction. In the deduction, (8) and (9) are the linchpin of the whole processing. By it, the goal of calculating g, the coregistration measure, with only three parts is fulfilled based on speckle statistics in a window of certain size $m \times n$.

For refined coregistration, the mask window moves with a step size of 0.1 pixels around the coarse coregistration position of the slave image to search for the optimal matching position. Alternatively, g is calculated only at integral grid and, then, is fitted with a quadratic function to find its maximum position.

In order to refine the coregistration precisely, we employ, for both the mask window of the master image and the matching window of the slave image, fringe contoured windows of $m \times n$ pixels, for which the phase term $\Delta\phi_c$ remains constant inside the windows [5]. As the two complex images of (1) and (2) are acquired from nearby positions, they are subject to a very similar random phase, inducing speckle noise that is strongly correlated when neglecting the temporal decorrelation effects. The subtraction of u_1 and u_2, Δu, thus results in a small difference that, on average, is narrowly and roughly symmetrically distributed around zero, whereas the values of u_1 and u_2 evenly range over the whole interval $[0 - 2\pi]$. If we again assume that the window size is not too small, and since sine is an odd function, the following is true:

$$\langle \sin \Delta u \rangle_{m\times n} = 0 \qquad \langle \cos \Delta u \rangle_{m\times n} \neq 0. \tag{14}$$

With (14) and $\Delta\phi_c =$ constant, in the contoured window, we obtain

$$\begin{aligned} &\langle \cos(\phi_{1c} - \phi_{2c} + u_1 - u_2)\rangle_{m\times n} \\ &\quad = \langle \cos(\Delta\phi_c + \Delta u)\rangle_{m\times n} \\ &\quad = \langle \cos\Delta\phi_c \cos\Delta u - \sin\Delta\phi_c \sin\Delta u\rangle_{m\times n} \\ &\quad = \cos\Delta\phi_c \langle \cos\Delta u\rangle_{m\times n} \end{aligned} \tag{15}$$

$$\begin{aligned} &\langle \sin(\phi_{1c} - \phi_{2c} + u_1 - u_2)\rangle_{m\times n} \\ &\quad = \langle \sin(\Delta\phi_c + \Delta u)\rangle_{m\times n} \\ &\quad = \langle \sin\Delta\phi_c \cos\Delta u + \cos\Delta\phi_c \sin\Delta u\rangle_{m\times n} \\ &\quad = \sin\Delta\phi_c \langle \cos\Delta u\rangle_{m\times n}. \end{aligned} \tag{16}$$

Substituting (15) and (16) in (12) results in

$$\begin{aligned} g &= \sqrt{C_1^2 + C_2^2} \\ &= \frac{|\langle A_1 A_2 \rangle_{m\times n}|}{\sqrt{\langle A_1^2 \rangle_{m\times n} \cdot \langle A_2^2 \rangle_{m\times n}}} \cdot \langle \cos\Delta u\rangle_{m\times n}. \end{aligned} \tag{17}$$

$$\begin{aligned} C_1 &= \frac{\langle A_1 A_2 \rangle_{m\times n} \cdot \langle \cos(\phi_{1c} + \phi_{2c} + u_1 + u_2) + \cos(\phi_{1c} - \phi_{2c} + u_1 - u_2)\rangle_{m\times n}}{\sqrt{\langle A_1^2 \rangle_{m\times n} \cdot \langle 1 + \cos(2\phi_{1c} + 2u_1)\rangle_{m\times n} \cdot \langle A_2^2 \rangle_{m\times n} \cdot \langle 1 + \cos(2\phi_{2c} + 2u_2)\rangle_{m\times n}}} \\ &= \frac{\langle A_1 A_2 \rangle_{m\times n}}{\sqrt{\langle A_1^2 \rangle_{m\times n} \cdot \langle A_2^2 \rangle_{m\times n}}} \cdot \langle \cos(\Delta\phi_c + \Delta u)\rangle_{m\times n} \end{aligned} \tag{10}$$

From (17), we observe a direct relation between the coregistration measure g and the noise Δu. It shows that the decorrelation noise Δu should approach zero when the two complex images are registered exactly as it is proportional to the degree of coregistration. The smaller Δu is, the larger the g and the better the coregistration. Thus, g can be used as the main criteria for coregistration of InSAR complex image pairs.

The main processing steps of the method are as follows.

1) Coarsely register the master image and the slave image based on the maximum of the coregistration quality-evaluation criterion g with square windows of size $m \times n$.
2) Generate phase image by the CCI method with square windows then determine the fringe-orientation map and fringe contoured windows [5]. The fringe contoured windows of equal phase coincide with the constant local phase of the fringe pattern [5], [6], [10].
3) Reregister the master image and the slave image based on the coregistration criterion g; this time with fringe contoured windows to refine the coregistration. The mask window moves with a step size of 0.1 or less pixels around the coarse coregistration position of the slave image to search for the optimal matching position. Both the window of the master image and the window of the slave image are fringe contoured windows of size $m \times n$.

III. Experimental Results

The effectiveness of the coregistration method proposed in this letter is demonstrated for the two pairs of SAR images. The first is a pair of C-band ERS-1/2 SAR images from orbits 41 125 and 21 452, over Kashgar area in China (baseline length = 49.88 m, 1999-05-27/28). The other datasets are from SIR-C/X-SAR (X-band, baseline length = 60 m, Mount Etna volcano, Italy).

The two pairs were both registered with the algorithm described above. The number of selected control points was 121. Fig. 1(a) and (b) shows the interferograms generated after coregistration with the proposed method. Fig. 1(a) displays adjacent parts of the scene, whereas Fig. 1(b) shows the identical area in upper and lower part. The upper parts of the two images are generated by the common complex conjugate multiplication, while the lower parts are computed by the CCI method [5]. The lower part of Fig. 1(a) is generated with the imaginary part of the slave image, while that of Fig. 1(b) is with the real part. It is clear to see that the interferograms derived by the CCI method are strongly speckle-noise-reduced.

Coherence is usually taken as the quantitative standard for evaluating the quality of the coregistration [11], [12]. To illustrate the improvement of the accuracy of InSAR image coregistration by means of the fringe contoured windows, we registered Kashgar area SAR images in four different ways: 1) three-part method with fringe contoured windows; 2) coherence method with fringe contoured windows; 3) three-part method with square windows; and 4) coherence method with square windows. For coregistration, the square windows were of size $7 \times 7 = 49$ pixels and the contoured windows of size $3 \times 15 = 45$ pixels. Taking both with approximately the same size avoids window-size effects. Finally, the coherence ρ of (13) was calculated for square windows of size 7×7 for all four ways of coregistration. The histograms of the calculated coherences are shown in Fig. 2. The residues of the interferograms generated after registration by the four different ways mentioned above—1)–4) are employed to evaluate the performances of the four registration methods. The residues of the methods of 1)–4) are 90 900, 87 400, 118 432, and 91 996, respectively. These results demonstrate the same conclusion as that of Fig. 2.

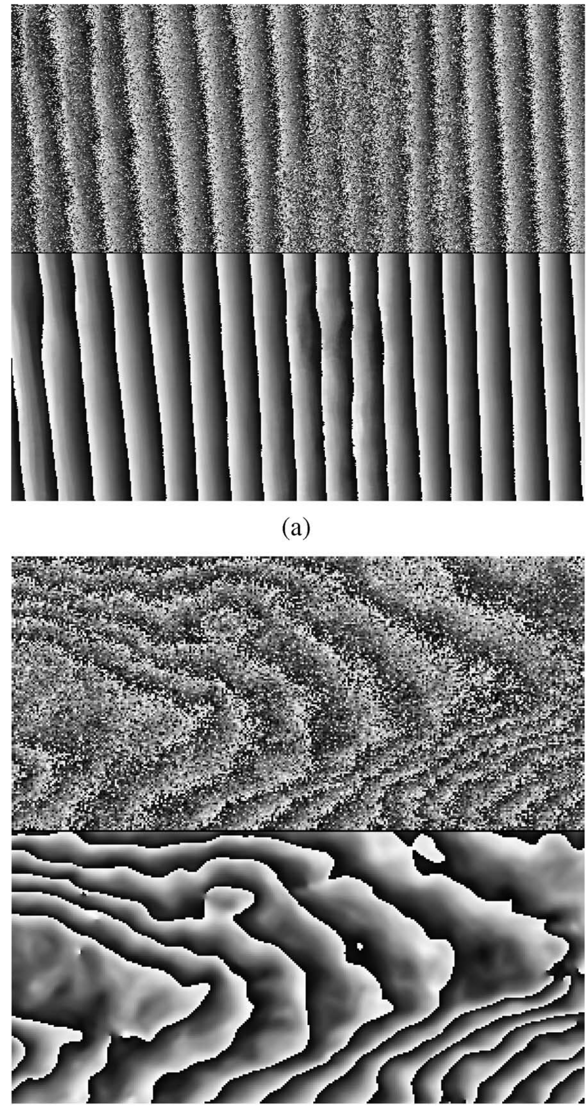

(a)

(b)

Fig. 1. Parts of the interferograms after the coregistration with our method generated by complex multiplication (upper part) and by the CCI method (lower part). (a) Displays adjacent parts of the scene (Kashgar area). (b) Shows the identical area (Mount Etna volcano area) in upper and lower part.

It is shown in Fig. 2 that our three-part method with contoured windows provides a better coherence than that derived by the widely used conventional four-part coherence method with square windows. The results exemplify the effectiveness of the method proposed in this letter and demonstrate that the method is very suitable for the coregistration of InSAR complex image pairs.

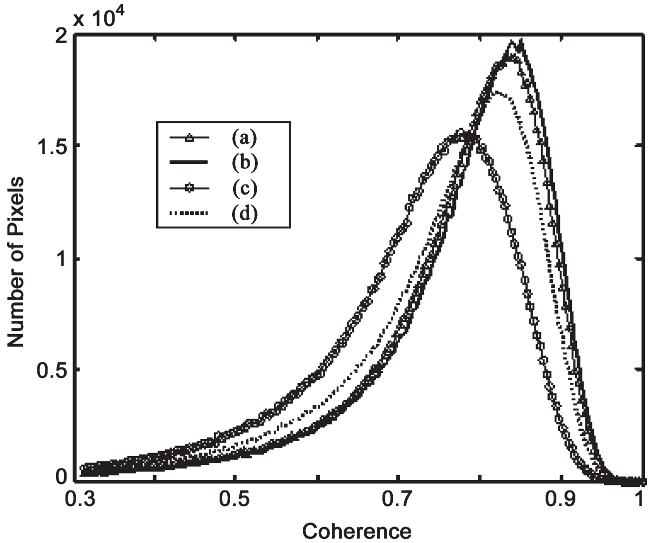

Fig. 2. Histograms of the coherence of the coregistration results obtained in four different ways. (a) Three-part method with fringe contoured window. (b) Coherence method with fringe contoured window. (c) Three-part method with squared window. (d) Coherence method with squared window.

Another important result given by Fig. 2 is that the existing four-part coherence method provides in conjunction with our contoured windows the best coregistration result, much better than that with square windows. Contoured windows are better adapted to the local topography of the scene and thus, the topography dependence in coregistration is circumvented. Using contoured windows instead of squared windows can overcome decreasing coregistration accuracy due to phase variations and help to achieve a higher accuracy for coregistration. It is easily understandable that the coherence method with contoured windows gives better result than the three-part method, because four parts of the two complex images contain more information compared to three parts. Therefore, we recommend employing contoured windows to increase the coregistration accuracy also for the existing coherence method.

IV. Conclusion

Three-part coregistration is proposed to register two interfering SAR images, with only three parts of the two complex images instead of four parts in the existing coregistration methods. Combined with our CCI phase image generation method proposed in [5], which can use only three parts of the two complex images to generate a speckle-noise-reduced phase image, three-part coregistration constitutes an integrated three-part InSAR data-processing chain. Without the three-part coregistration, the CCI method is not a real three-part method and is less important. If the spaceborne SAR imaging process is implemented on the satellite, with our integrated methods of coregistration and phase-image generation, only three quarter of the data are needed to be transmitted back to the ground to conduct InSAR data processing, which is a significant advantage over existing methods.

Finally, contoured windows have been shown to be very beneficial for the three-part coregistration, as well as for existing coherence methods, since they can decrease the influence of phase variation. We, therefore, recommend that existing coherence methods should also try to use contoured windows to increase the accuracy of the coregistration. Our future work is directed toward the development of robust adaptive algorithms to retrieve high-quality contoured windows.

References

[1] P. A. Rosen *et al.*, “Synthetic aperture radar interferometry,” *Proc. IEEE*, vol. 33, no. 3, pp. 333–382, Mar. 2000.

[2] Q. Lin, J. F. Vesecky, and H. A. Zebker, “New approaches in interferometric SAR data processing,” *IEEE Trans. Geosci. Remote Sens.*, vol. 30, no. 3, pp. 560–567, May 1992.

[3] F. K. Li and R. M. Goldstein, “Studies of multibaseline spaceborne interferometric synthetic aperture radars,” *IEEE Trans. Geosci. Remote Sens.*, vol. 28, no. 1, pp. 88–97, Jan. 1990.

[4] A. K. Gabriel and R. M. Goldstein, “Crossed orbit interferometry: Theory and experimental results from SIB-B,” *Int. J. Remote Sens.*, vol. 9, no. 5, pp. 857–872, 1988.

[5] Q. Yu, S. Fu, H. Mayer, X. Liu, X. Yang, and Z. Lei, “Generation of speckle-reduced phase images from three complex parts for synthetic aperture radar interferometry,” *Appl. Phys. Lett.*, vol. 88, no. 11, p. 114106, Mar. 2006.

[6] Q. Yu, X. Yang, S. Fu, X. Liu, and X. Sun, “An adaptive contoured window filter for interferometric synthetic aperture radar,” *IEEE Geosci. Remote Sens. Lett.*, vol. 4, no. 1, pp. 23–26, Jan. 2007.

[7] R. Bamler and P. Hartl, “Synthetic aperture radar interferometry,” *Inverse Probl.*, vol. 14, no. 4, pp. 1–54, 1998.

[8] J. W. Goodman, *Laser Speckle and Related Phenomena*. New York: Springer-Verlag, 1975.

[9] C. Lopez-Martinez and E. Pottier, “Coherence estimation in SAR data based on speckle noise modeling,” *Appl. Opt.*, vol. 46, no. 4, pp. 544–558, Feb. 2007.

[10] Q. Yu, X. Sun, X. Liu, X. Ding, and Z. Qiu, “Removing speckle noise and skeleton extraction from a single speckle fringe pattern,” *Opt. Eng.*, vol. 42, no. 1, pp. 68–74, 2003.

[11] H. A. Zebker and J. Villasenor, “Decorrelation in interferometric radar echoes,” *IEEE Trans. Geosci. Remote Sens.*, vol. 30, no. 5, pp. 950–959, Sep. 1992.

[12] J. Askne and J. O. Hagberg, “Potential of interferometric SAR for classification of land surfaces,” in *Proc. Int. Geosci. and Remote Sens. Symp.*, Tokyo, Japan, 1993, pp. 985–987.